JOURNAL OF MATERIALS SCIENCE 28 (1993) 2955–2961

Failure mechanism of chromium–silicon–oxide resistive films stressed by electric pulse loading

K. SATO, T. NAGATA, M. WATANABE
Mechanical Engineering Research Laboratory, Hitachi Ltd, 502, Kandatsu, Tsuchiura, Ibaraki, Japan
H. NAKAYAMA
Telecommunications Division, Hitachi Ltd, 216, Totsuka, Yokohama, Kanagawa, Japan

The failure mechanism of chromium–silicon–oxide (Cr–Si–O) resistive films stressed by electric pulse loading has been investigated. Cr–Si–O resistive films were deposited with the Cr–Si target in an oxygen partial pressure of 0.05 Pa by reactive sputtering. The composition was 26 at% Cr, 48 at% Si, and 26 at% O with a microstructure of $CrSi_2$ small crystallites and an amorphous SiO_2 matrix. Resistance increased and flow patterns on the film surfaces were observed during the load–life tests to stress the resistive films at high-power electric pulses. The temperature increase in the film during the load–life tests was obtained numerically by using a finite element method (FEM), due to the difficulty of experimentally measuring the temperature increase. It reaches 400 °C, for example, when supplied with a 0.5 W electric pulse of 1 ms pulse width. Film lifetimes and peak temperatures have a linear relation in the Arrhenius plots. Structurally, a decrease of chromium concentration was observed near the cathode region after electric pulse loading. These results indicate that the $CrSi_2$ particles move in the Cr–Si–O film during the load–life tests. This movement induces the resistance increase and the final failure of the film as the electromigration phenomenon in pure aluminium or aluminium alloy films induces film failure. The activation energy for the electromigration of $CrSi_2$ particles in the Cr–Si–O film was found to be 1.53 eV from the slopes in the Arrhenius plots.

1. Introduction

Thin-film resistors are required in many integrated circuit applications. Cr–Si–O films have been investigated since 1960 as a material for microelectronic resistors [1, 2]. In the early 1960s, the reported electrical properties of seemingly identical films varied widely because with the existing deposition processes, the film composition could not be reproduced accurately [3, 4]. In the late 1960s, the improvement of deposition techniques made it possible to obtain well-defined Cr–Si–O or Cr–Si films. The structures and several electrical properties were investigated on Cr–Si–O films deposited by flash-evaporation [5] and Cr–Si films deposited by electron-beam heating [6]. Cr–Si–O films have recently begun to be used in high-power devices such as thermal print heads [7, 8]. As a result, their stability against electric power loading or exposure to high temperatures has been investigated, as well as their structures and electrical properties.

This paper describes a reliability study of Cr–Si–O resistive films deposited by reactive sputtering. The failure mechanism of Cr–Si–O films stressed by high-power electric pulses was investigated by resistance change measurements, numerical simulations of film temperature increases, and X-ray micro-analysis (XMA).

2. Experimental procedure

2.1. Sample preparation

Cr–Si–O films were deposited by reactive sputtering on Al_2O_3 substrates which were covered with a 60 μm thick glaze layer composed mainly of SiO_2 and PbO. These glaze layers efficiently increased the temperature of the Cr–Si–O films [9], and aided adhesion of the Cr–Si–O films to the Al_2O_3 substrate. High-purity silicon (99.999%) and chromium (99.97%) were used as source materials for Cr–Si–O film depositions. The sputtering target was made of a chromium ingot with surface grooves and silicon slices embedded in the grooves. The films were deposited to a thickness of 0.1 μm in an oxygen partial pressure of 0.05 Pa after evacuating the sputtering system to 7×10^{-5} Pa. The substrate temperature during deposition ranged from 130–170 °C. The deposition rate was 1.7 nm min^{-1}. After the deposition of the Cr–Si–O film, chromium was deposited to a thickness of 0.3 μm on the Cr–Si–O film before depositing the aluminium conductive film. The Cr–Si–O film is known to react with the aluminium film and to make a low-resistivity region that migrates into the resistor area between the two films [6]. The chromium film was able to prevent this reaction. After the deposition of the chromium film, aluminium was deposited as a conductive layer

0022-2461 © *1993 Chapman & Hall*

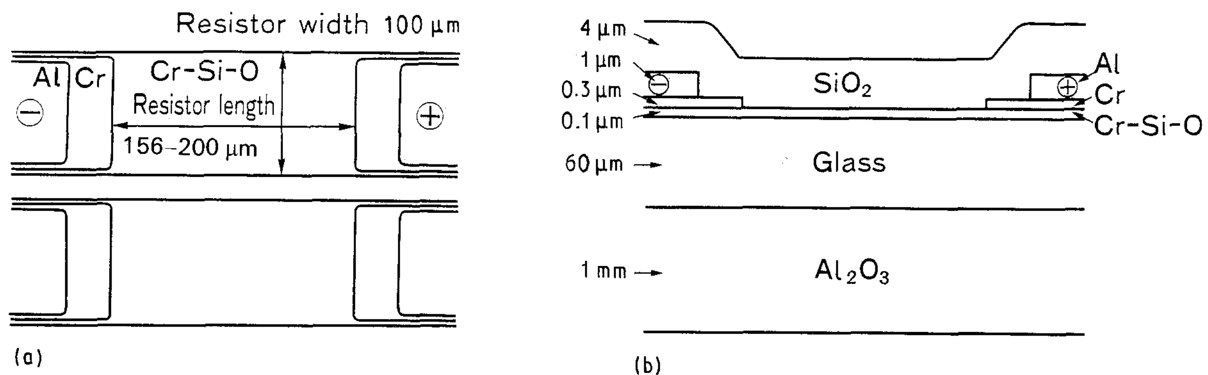

Figure 1 Schematic diagram of a specimen for the load–life test. (a) Top view, (b) cross-sectional view.

to a thickness of 1 µm. Subsequently, aluminium, chromium and Cr–Si–O films were patterned one after another by using a common photolithography process. The Cr–Si–O resistors were 100 µm in width and ranged in length from 156–200 µm. The aluminium electrode films were separated from the resistors by distances ranging from 30–40 µm by the chromium films. The specimen after etching is shown in Fig. 1a. The specimen was then covered with a 4 µm thick SiO_2 passivation film deposited by a sputtering method. A diagram of the cross-section of the specimen is shown in Fig. 1b. The specimen was annealed at 350 °C for 1 h in air before the load–life tests to stabilize the characteristics as a thin-film resistor.

Resistance measurements were made at room temperature before the experiments. Data for the three types of specimens (resistor lengths: (1) 156 µm, (2) 179 µm, and (3) 200 µm) are listed in Table I. Resistivity of the Cr–Si–O films was 0.0029 Ω cm, on average.

The composition of the Cr–Si–O film was studied by XMA and found to be 26 at % Cr, 48 at % Si, and 26 at % O. The X-ray diffraction pattern of the Cr–Si–O film is shown in Fig. 2. Broad and obscure peaks of $SiO_2(1\,0\,1)$ and $CrSi_2(1\,1\,1)$ observed in this diagram indicate that the principal structures of the Cr–Si–O film are SiO_2 and $CrSi_2$ that are almost amorphous or small grains. Cr_3Si and Cr_5Si_3 have been reported to be conductive components in annealed Cr–Si–O films containing 50 at % SiO [5]. Because the Cr–Si–O films examined here contained as much as 74 at % SiO, the other silicide, $CrSi_2$, is thought to be a major conductive component. The microstructure of the Cr–Si–O film was observed by using transmission electron microscopy (TEM). From the transmission electron micrograph and the diffraction pattern shown in Fig. 3, it was found that $CrSi_2$ was crystalline and that its grains ranged from 30–140 nm in diameter. These $CrSi_2$ small grains seemed to be surrounded by an SiO_2 matrix like that observed on the Cr–Si–O film containing 50 at % SiO [5].

TABLE I Resistance and resistivity of three types of specimen

	Resistor length (µm)		
	156	179	200
Average resistance (Ω)	444	548	560
Resistivity (Ω cm)	0.0028	0.0031	0.0028

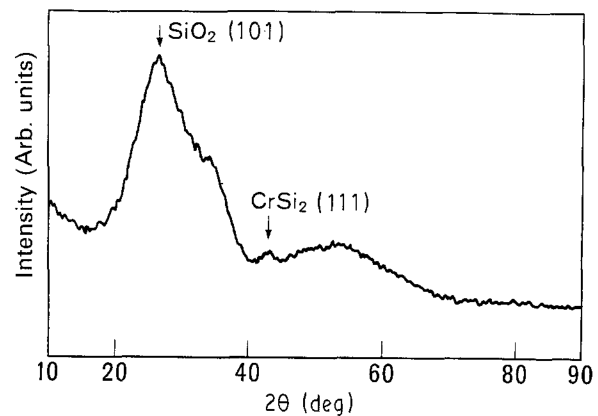

Figure 2 X-ray diffraction pattern of Cr–Si–O resistive film.

2.2. Experimental conditions

Three types of specimen were prepared with resistor lengths of (1) 156 µm, (2) 179 µm, and (3) 200 µm. In the load–life tests these resistive films were stressed by high-power electric pulses of 1 ms pulse width with a 5 ms pulse cycle. Resistance-change measurements and surface observations were carried out during the experiments. The lifetime, defined as the total pulse counts when the resistance changed to 10% of its initial value, was determined for each resistive film. This failure criterion is reasonable when these resistive films are used for electric devices [10]. Unless they failed earlier, the resistive films were stressed by 1.5×10^8 pulses. The voltage of the electric pulse, V, was decided by the initial resistance, R_0 and input power, W, by using the following equation

$$V = (WR_0)^{1/2} \qquad (1)$$

This voltage was kept constant during the experiment to make the experiment easier. The input power ranged from 0.425–0.75 W. Although the real input power decreased a little during the experiment with the resistance increase of the resistive film, the decrease was negligible. Specimens were placed on the aluminium plates at 20, 50, or 70 °C during the experiments.

After the load–life tests, the surfaces of the resistive films were observed with an optical microscope, and a constituent analysis of the resistive film was done after removing the SiO_2 passivation film by XMA.

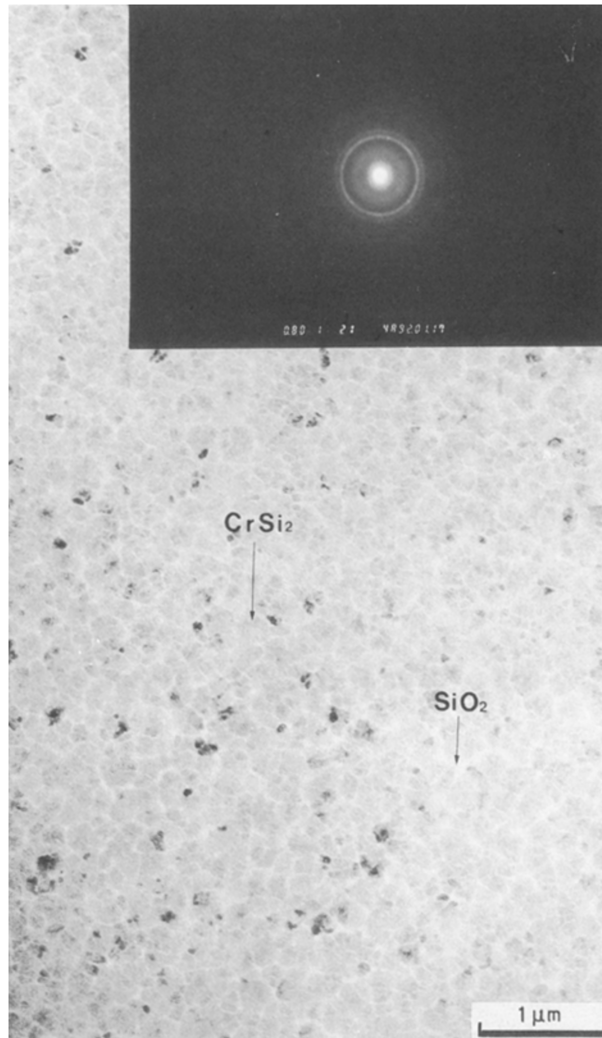

Figure 3 Transmission electron micrograph and diffraction pattern of Cr–Si–O resistive film.

3. Results and discussion

3.1. Load–life test

Fig. 4 shows the resistance changes for 200 μm long resistors stressed by electric pulses from 0.55–0.75 W. They were normalized by the initial resistance, R_0. Each data plotted in this figure was the average resistance of five resistors. The specimens were put on the aluminium plates at 20 °C during the load–life tests. The resistance gradually increased for the resistors stressed by 0.55, 0.575, 0.65, 0.70, and 0.75 W electric pulses. Failure occurred within 1.5×10^7 pulses for those resistors stressed by electric pulses of more than 0.65 W. However, small resistance decreases were observed after reaching a peak value above a 10% resistance increase for the resistors stressed by 0.60 and 0.625 W electric pulses. The lifetime, defined as the total pulse counts when the resistance increased to 10% of its initial value, was determined by the resistance change measurements shown in Fig. 4.

Optical micrographs of the resistor surfaces stressed by those electric pulses are shown in Fig. 5. No distinct colour change was recognizable on the surface of the resistor stressed by 0.55 W electric pulses. However, a small stream-like pattern appeared near the cathode region of the resistor stressed by 0.575 W electric pulses, and the stream pattern became larger in those resistors stressed by 0.60 and 0.625 W electric pulses. This stream pattern seemed to be a migration trace of some substance from the cathode region to the anode region. The resistors stressed by 0.65 and 0.70 W electric pulses broke after 1.5×10^7 pulses and 1.0×10^7 pulses, respectively. These two resistive films had large voids in them. From the micrographs shown in Fig. 5, these voids were found to be formed after the stream pattern developed, as explained above. The lifetimes of three types of specimens stressed by electric pulses ranging from 0.425–0.70 W are shown in Fig. 6. From this figure, it was observed that the lifetime depended on both resistor length and input electric power, and that a longer resistor had a longer lifetime.

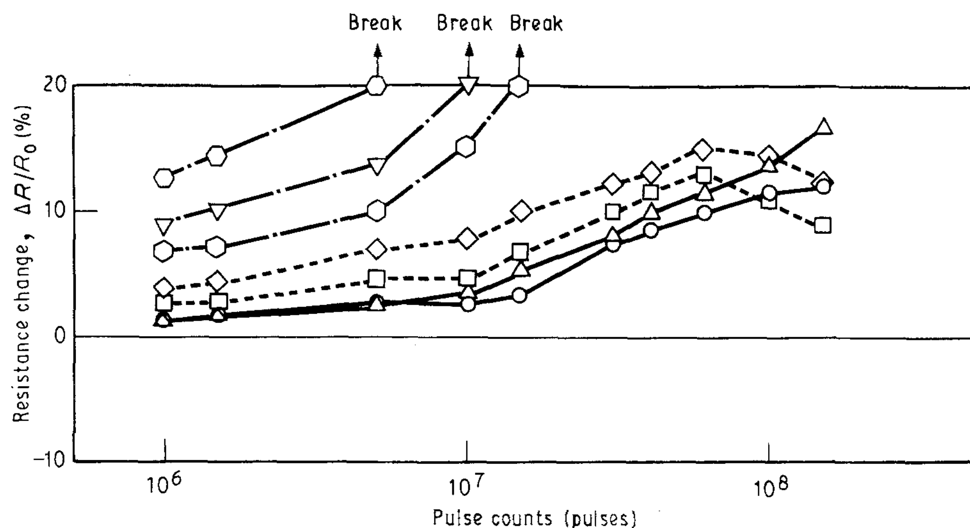

Figure 4 Resistance changes of Cr–Si–O resistive films stressed at various electric pulses, resistor length = 200 μm. Input power (W): (○) 0.55, (△) 0.575, (□) 0.60, (◇) 0.625, (⬡) 0.65, (▽) 0.70, (⬠) 0.75.

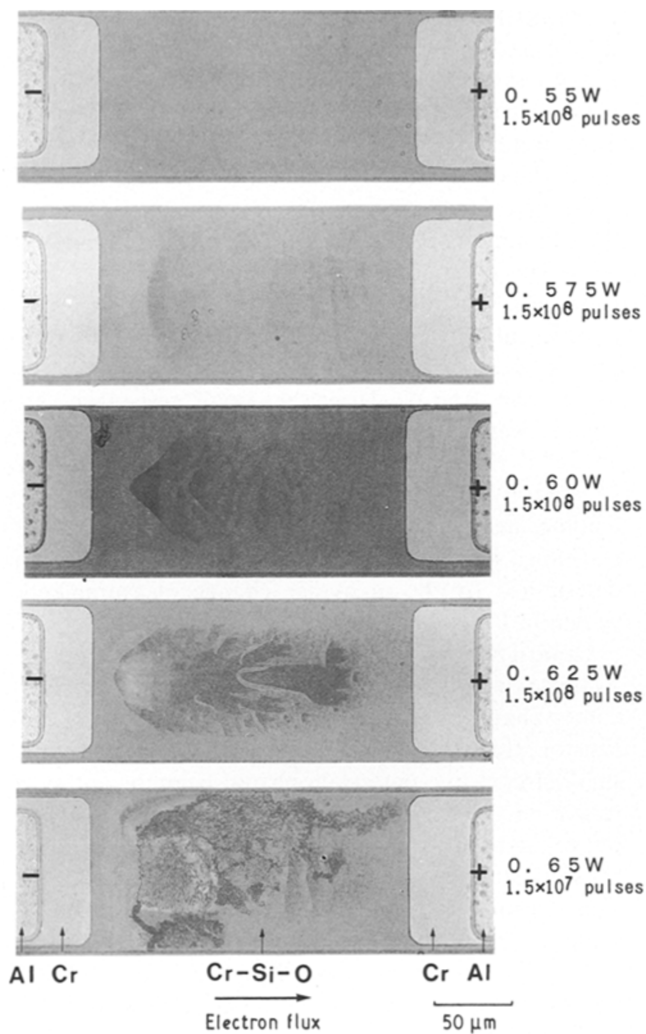

Figure 5 Optical micrographs of Cr–Si–O resistive films stressed at electric pulses; resistor length = 200 µm.

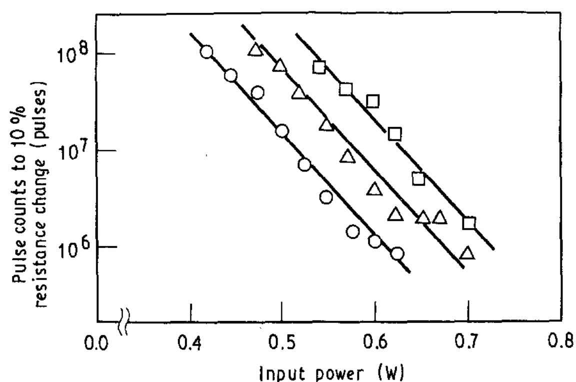

Figure 6 Relation between input power and pulse counts to 10% resistance change for three types of specimen with resistor lengths of (○) 156 µm, (△) 179 µm and (□) 200 µm.

3.2. Numerical simulation of temperature increase

It is very difficult to experimentally measure the temperature increase of a thin-film resistor when an electric pulse is supplied to the resistor and, as a result, several methods, such as a finite element method, differential method, and network method have been applied as a solution [9–11]. The three-dimensional finite element method was used in this research.

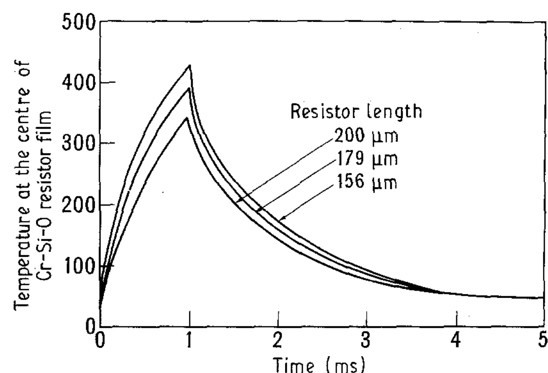

Figure 7 Temperature dynamics at the centre of resistors stressed at a 0.5 W electric pulse of 1 ms pulse width calculated by FEM; resistor length = 156 µm, 179 µm and 200 µm.

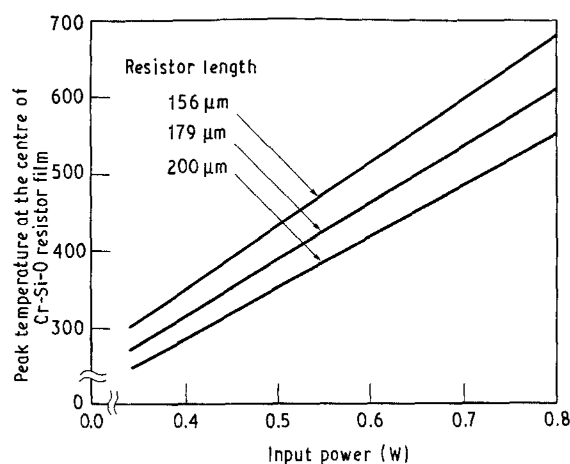

Figure 8 Relation between peak temperature at the centre of resistors and input electric power.

Fig. 7 shows the temperature dynamics at the centre of three types of resistors stressed by a 0.5 W electric pulse of 1 ms pulse width. The initial temperature was set at 20 °C for this simulation. The temperature rapidly increased to the peak value of about 400 °C and cooled down relatively slowly to the initial temperature. Furthermore, it was found that a higher peak temperature was achieved for a shorter resistor.

The relation between the peak temperature after 1 ms heating and the electric power input is shown in Fig. 8. From this figure it is possible to obtain the peak temperature at the centre of three types of resistors during the load–life tests.

3.3. Relation between lifetime and temperature

Fig. 9 is the Arrhenius plot to show the relation between the lifetimes determined by the load–life tests shown in Fig. 6, and the peak temperatures at the centre of the resistors shown in Fig. 8 for three types of resistors stressed by electric pulses ranging from 0.425–0.7 W. Although the peak temperature changed a little during the load–life tests due to the increase of resistance, the change was negligible. From Fig. 9, it was observed that the resistors with the same peak temperatures had the same lifetimes in the load–life

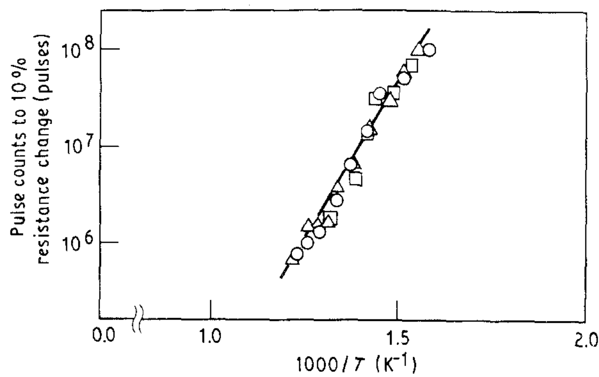

Figure 9 Arrhenius plots to show the relation between lifetimes and peak temperatures for three types of specimen of resistor lengths = (○) 156 μm, (△) 179 μm, and (□) 200 μm.

tests in spite of the difference of resistor length. Furthermore, it was observed that the logarithm of lifetimes had a linear relation with the inverse of the peak temperatures.

This type of relation is well known in electromigration phenomena which are the primary cause for the failure of aluminium or aluminium alloy interconnects in microelectronics [12–14]. The results of the mean time to failure (MTF) of aluminium or aluminium alloy films in the electromigration experiments are interpreted by the following formula developed by Black [12]

$$\mathrm{MTF} = Aj^{-m}\exp(Q/kT) \quad (2)$$

Where A is a constant, j is the current density, m is a power of j (usually $m = 2$), Q is the activation energy, k is Boltzmann's constant, and T is the absolute film temperature. From Equation 2, the following equation is derived.

$$\log(\mathrm{MTF}) = \log(Aj^{-m}) + Q/kT \quad (3)$$

The slope of the straight line in Arrhenius plots gives the activation energy for electromigration damage. The absolute film temperature was not actually constant in the experiments shown in Fig. 7, because the Cr–Si–O resistive films were stressed by pulse-like current. The peak temperatures were used for the film temperatures in our analysis.

The lifetime against electromigration damage is a function of the current density passing through the film, as well as the temperature of the film. The range of the current densities passing through the Cr–Si–O resistive films in the load–life tests is shown in Table II. The small changes in the current densities due to the resistance increases were negligible during the load–life tests. The data in Fig. 9 were not obtained under the same current density conditions as shown in Table II. Additional load–life tests were carried out to make the analysis of the failure mechanism more accurate. Only the 200 μm resistor length specimens were used. They were placed on the aluminium plates at 20, 50 and 70 °C during the load–life tests. The resistors were stressed at high-power electric pulses of 1 ms pulse width with a 5 ms pulse cycle from 0.5–0.7 W.

TABLE II Range of current density in the load–life test

	Resistor length (μm)		
	156	179	200
Input power (W)	0.425–0.625	0.475–0.7	0.55–0.7
Current density (10^5 A cm^{-2})	3.1–3.8	3.1–3.8	3.1–3.8

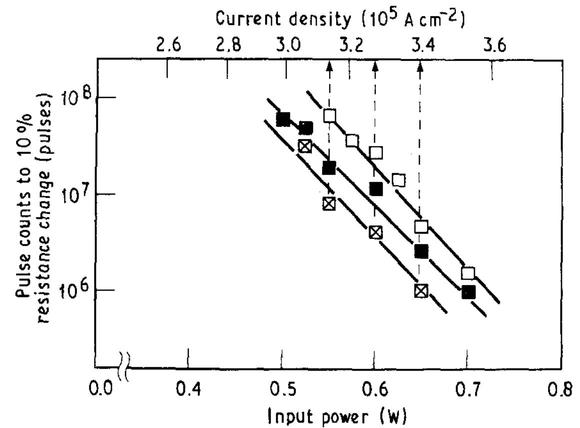

Figure 10 Relation between input power and pulse counts to 10% resistance change at three different substrate temperatures: (□) 20 °C, (■) 50 °C, (□) 70 °C. Resistor length = 200 μm.

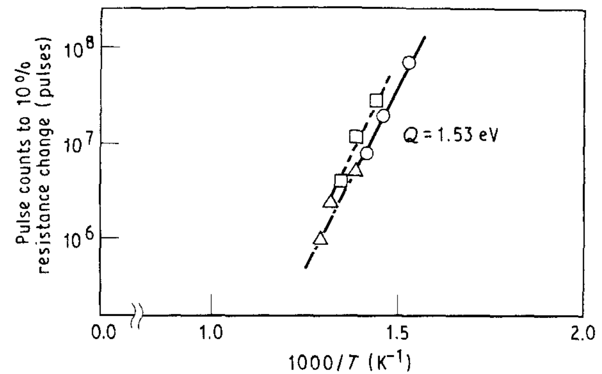

Figure 11 Arrhenius plots to show the relation between lifetimes and peak temperatures for 200 μm long resistors at three different current densities: (○) 3.13 × 10^5A cm^{-2}, (□) 3.27 × 10^5 A cm^{-2}, (△) 3.40 × 10^5 A cm^{-2}.

Fig. 10 shows the results of these load–life tests. The relation between the lifetimes and the peak temperatures of the Cr–Si–O films under the same current density conditions were obtained from these results. The peak temperatures when the aluminium plates were at 50 or 70 °C were calculated by setting the initial temperature for 50 or 70 °C in the simulation, respectively. Fig. 11 is the Arrhenius plots of the lifetimes and the peak temperatures for the Cr–Si–O resistive films stressed at 3.13, 3.27, and 3.40 × 10^5 A cm^{-2}. Although the dependence of lifetimes on current densities was not clearly observed under current densities ranging from 3.13–3.40 × 10^5 A cm^{-2}, the distinct linear relation between the logarithm of lifetimes and the inverse of the peak temperatures was achieved under the same current density conditions.

From this figure, it was found that the failure mechanism of Cr–Si–O resistive films stressed at high-power electric pulses was quite similar to the electromigration damage. The activation energy obtained from the slope of those straight lines was 1.53 eV.

3.4. Change of Cr–Si–O film composition due to electric pulse loading

X-ray micro-analysis was performed to determine the change of the film composition after pulse loading. The measured specimen was a Cr–Si–O resistive film 200 μm long, stressed by 1×10^7 pulses of 1 ms pulse width with a 5 ms pulse cycle and 0.6 W electric power. After the pulse loading, the SiO_2 passivation film thickness was reduced to 0.3 μm by argon ion sputtering. The composition of the Cr–Si–O resistive film was then analysed through the passivation film. The intensity ratios of CrK_α peak to SiK_α peak are shown in Fig. 12. The silicon peaks are from the SiO_2 passivation film, the Cr–Si–O film, and the glaze layer on the Al_2O_3 substrate. The measurements were carried out along the centre line of the Cr–Si–O film as shown in Fig. 12. From this figure, it was found that the concentration of chromium decreased 10–40 μm from the chromium cathode. This position corresponded to where the stream pattern began to appear during the load–life test.

During an electromigration experiment on aluminium or aluminium alloy films, the film was heated by joule heating according to the thermal characteristics of the experimental system, with a temperature variation along the stripe induced similar to the Cr–Si–O resistive films during the load–life tests. The velocity of the moving aluminium atom is a strong function of the temperature, and therefore the temperature variation induces a velocity variation along the stripe. The divergence of this velocity field is responsible for local depletions or accumulations of the moving aluminium atom [15]. Many voids were observed in the cathode region because the depletions were larger in the cathode region where the temperature gradient was steep. On the other hand, many hillocks were observed in the anode region where the temperature gradient was steep, due to larger accumulations [16]. The chromium concentration decrease observed near the cathode region is thought to be induced by electromigration in the Cr–Si–O resistive film, as many voids are formed near the cathode region in the aluminium films. The moving substance is thought to be $CrSi_2$ particles because the Cr–Si–O film is composed of small crystallites of $CrSi_2$ and the SiO_2 matrix.

The temperature profile along the 200 μm long Cr–Si–O resistive film stressed by an electric pulse of 0.5 W is shown in Fig. 13. This result was obtained by numerical simulation using a three-dimensional finite element method. From Fig. 13, it can be seen that the temperature gradient in the Cr–Si–O resistive film was steepest in the region 10–40 μm from the chromium electrode. Therefore, the depletion of the moving $CrSi_2$ particles by electromigration was largest in the region near the chromium cathode, and it induced the chromium concentration decrease.

The resistance increase of specimens during the load–life tests was also found to be induced by the electromigration of $CrSi_2$ particles. This is because the depletion of $CrSi_2$, the dominant conducting component in the Cr–Si–O films, made the local resistivity very large. This local resistivity increase was confirmed by temperature distribution measurements. Fig. 14 shows the temperature distribution of a 200 μm long Cr–Si–O resistive film measured with an infrared thermometer. Fig. 14a and b show temperature distribution before the load–life test and after a 1×10^7 pulse load of 0.6 W, respectively. A constant electric power of 0.185 W was supplied to those specimens, during the measurements. It was not easy to calibrate the temperature measured with an infrared thermometer, and therefore only the qualitative measurements were carried out. The spot size of the infrared thermometer was 35 μm diameter. Although the temperature distribution was symmetrical for the

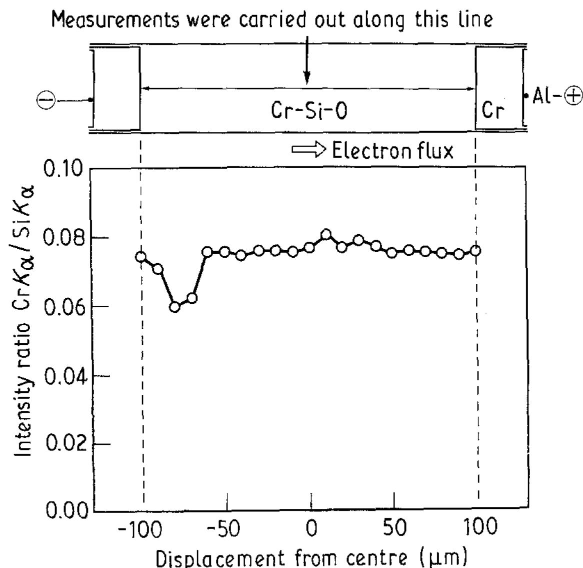

Figure 12 Intensity ratio of CrK_α to SiK_α in Cr–Si–O resistive film after pulse loading measured by XMA. Resistor length = 200 μm, input power = 0.6 W, pulse counts = 1×10^7 pulses.

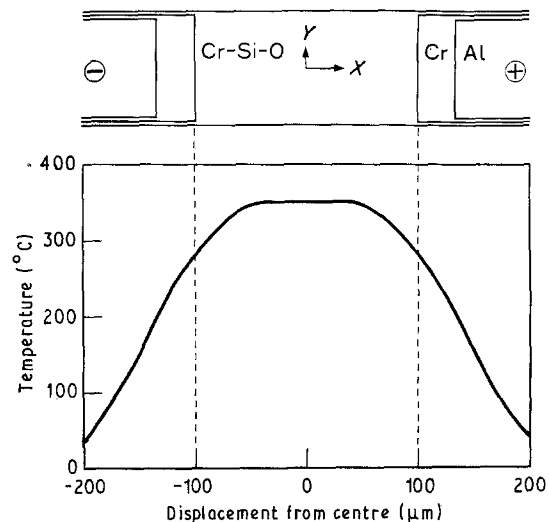

Figure 13 Temperature profile of Cr–Si–O resistive film stressed at a 0.5 W electric pulse of 1 ms pulse width calculated by FEM.

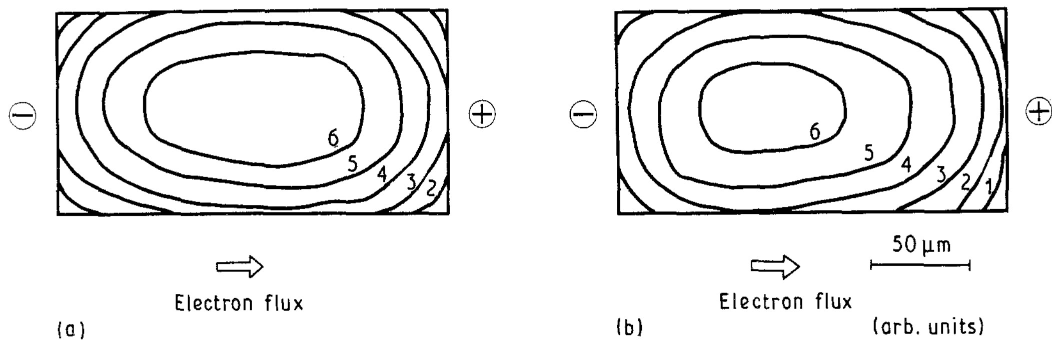

Figure 14 Temperature distributions of Cr–Si–O resistive films (a) before and (b) after pulse loading measured by infrared thermometer. Resistor length = 200 µm, input power = 0.6 W, pulse counts = 1×10^7 pulses.

Cr–Si–O resistive film before the load–life test, the peak temperature was observed in the region near the cathode for the film stressed by the electric pulses. This result indicates that resistivity near the cathode region of the film was larger than that near the anode region.

4. Conclusions

Cr–Si–O resistive films were deposited from chromium and silicon targets in an oxygen partial pressure of 0.05 Pa by a reactive sputtering method, and their failure mechanism in load–life tests was investigated. This work leads to the following conclusions.

1. The composition of this Cr–Si–O resistive film was 26 at% Cr, 48 at% Si, and 26 at% O. Its microstructure was composed of very small $CrSi_2$ crystallites and amorphous SiO_2 matrix. Its resistivity ranged from 0.0028–0.0031 Ω cm.

2. The resistance increase of the Cr–Si–O resistive film during load–life tests was induced by a chromium concentration decrease near the cathode region due to the electromigration of $CrSi_2$ particles.

3. Lifetimes and peak temperatures of Cr–Si–O resistive films in the load–life tests had a good linear relation in the Arrhenius plots. The slopes of the lines show the activation energy to be 1.53 eV for the $CrSi_2$ electromigration.

Acknowledgements

The authors thank Mr Hiratsuka and Mr Morita, Telecommunications Division of Hitachi Ltd, for their helpful cooperation and suggestions.

References

1. M. BECKERMAN and R. E. THUN, in "Transactions of the 8th AVS Vacuum Symposium" (Pergamon Press, New York, 1961) p. 905.
2. W. J. OSTRANDER and C. W. LEWIS, *ibid*., p. 881.
3. M. BECKERMAN and R. L. BULLARD, in "IEEE Proceedings of the 1962 Electronic Components Conference" (1962) p. 53.
4. R. WAGNER and K. M. MERZ, in "IEEE Proceedings of the 1964 Electron Components Conference" (1964) p. 97.
5. R. GLANG, R. A. HOLMWOOD and S. R. HERD, *J. Vac. Sci. Technol.* **4**(4) (1967) 163.
6. R. K. WAITS, *Trans. Metall. Soc. AIME* **242** (1968) 490.
7. T. KAMEI, M. MITANI, K. ABE, Y. KAWAHITO, S. HIRATSUKA, K. KURIHARA, H. ANDO and T. NISHIDA, in "IEEE Proceedings of the 1982 Electronic Components Conference" (1982) p. 481.
8. T. KAMEI, M. MITANI, T. KAWAHITO, T. ISOGAI, M. TANAKA, S. HIRATSUKA, K. KURIHARA and H. ANDO, in "Proceedings of the International Symposium on Microelectronics, ISHM '82" (ISHM, Virginia, 1982) p. 320.
9. M. ISHIZUKA, in "IEEE/CHMT '89 Japan IEMT Symposium" (1989) p. 311.
10. T. NAGATA, M. WATANABE and S. HIRATSUKA, in "Proceedings of the International Symposium on Microelectronics, ISHM '87" (ISHM, Virginia 1987) p. 207.
11. S. HIRANO, K. IBATA, T. TOYOSAWA and K. TOGAWA, in "Proceedings of the International Symposium on Microelectronics, ISHM '88" (ISHM, Virginia 1988) p. 480.
12. J. R. BLACK, *Proc. IEEE* **59** (1969) 1587.
13. R. E. JONES Jr and L. D. SMITH *J. Appl. Phys.* **61** (1987) 4670.
14. J. CHO and C. V. THOMPSON, *J. Electron. Mater.* **19** (1990) 1207.
15. R. E. HUMMEL, R. T. DEHOFF and H. J. GEIER, *J. Phys. Chem. Solids* **37** (1976) 73.
16. C. Y. CHANG and R. W. VOOK, *J. Mater. Res.* **4** (1989) 1172.

Received 3 March
and accepted 5 November 1992